Lawrence Berkeley National Laboratory

Title
The hunt for the third acceptor in CuInSe2 and Cu(In,Ga)Se2 absorber layers

Permalink
https://escholarship.org/uc/item/790156f0

Authors
Babbe, Finn
Elanzeery, Hossam
Wolter, Max H
et al.

Peer reviewed

The hunt for the third acceptor in CuInSe$_2$ and Cu(In,Ga)Se$_2$ absorber layers

Finn Babbe[1,2] , Hossam Elanzeery[1] , Max H Wolter[1] , Korra Santhosh[1,3] and Susanne Siebentritt[1]

[1] Laboratory for Photovoltaics, Physics and Material Science Research Unit, University of Luxembourg, 41, Rue de Brill, L-4422 Belvaux, Luxembourg
[2] Joint Center for Artificial Photosynthesis, Lawrence Berkeley National Laboratory, 1 Cyclotron Road, 94720 Berkeley CA, United States of America

E-mail: FinnBabbe@lbl.gov

CrossMark

Abstract

The model for intrinsic defects in Cu(In,Ga)Se$_2$ semiconductor layers is still under debate for the full range between CuInSe$_2$ and CuGaSe$_2$. It is commonly agreed by theory and experiment, that there are at least one shallow donor and two shallow acceptors. Spatially resolved photoluminescence on CuGaSe$_2$ previously revealed a third acceptor. In this study we show with the same method that the photoluminescence peak at 0.94 eV in CuInSe$_2$, previously attributed to a third acceptor, is a phonon replica. However another pronounced peak at 0.9 eV is detected on polycrystalline CuInSe$_2$ samples grown with high copper and selenium excess. Intensity and temperature dependent photoluminescence measurements reveal that this peak originates from a DA-transition from a shallow donor (<8 meV) into a shallow acceptor A3 (135 ± 10) meV. The DA3 transition has three distinct phonon replicas with 28 meV spectral spacing and a Huang Rhys factor of 0.75. Complementary admittance measurements are dominated by one main step with an activation energy of 125 meV which corresponds well with the found A3 defect. The same defect is also observed in Cu(In,Ga)Se$_2$ samples with low gallium content. For [Ga]/([Ga] + [In])-ratios of up to 0.15 both methods show a concordant increase of the activation energy with increasing gallium content shifting the defect deeper into the bandgap. The indium vacancy V_{In} is discussed as a possible origin of the third acceptor level in CuInSe$_2$ and V_{III} in Cu(In,Ga)Se$_2$.

Keywords: photoluminescence, defects, CIGS, admittance, CuInSe$_2$, Cu-rich

S Supplementary material for this article is available online

(Some figures may appear in colour only in the online journal)

Introduction

Solar cells made from chalcopyrite absorber layers Cu(In,Ga)Se$_2$ (CIGS) achieve the highest power conversion efficiencies of all thin film solar cells, reaching up to 23.3 % [1, 2]. From optical measurements (photoluminescence (PL) [3–6] and

cathodoluminescence (CL) [3, 7]) as well as electrical measurements (admittance [8], Hall [9, 10]) a defect model was derived for the ternaries CuInSe$_2$ and CuGaSe$_2$ as well as partly for Cu(In,Ga)Se$_2$. A recent review can be found in [11]. For CuInSe$_2$ the model includes a shallow donor ($E_D = (6$-$10)$ meV) and two shallow acceptor with $(E_{A1,CIS} = 40$ meV) and $(E_{A2,CIS} = 60$ meV) [4]. With the addition of gallium the activation energy of the donor level changes only negligible, whereas both acceptors continuously shift deeper into the bandgap resulting in higher activation energies in CuGaSe$_2$ $((E_{A1,CGS} = 60$ meV) and $(E_{A2,CGS} = 100$ meV)) [6]. A third

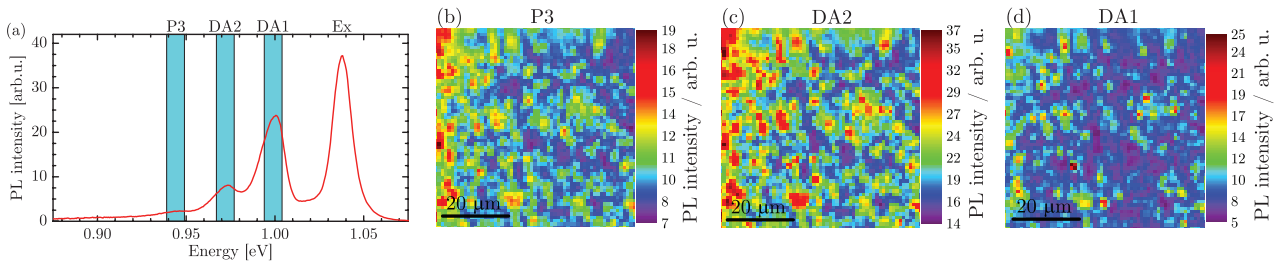[3] On leave from: Indian Institute of Technology—Bombay, India

Figure 1. (a) Photoluminescence spectra of a polycrystalline CuInSe$_2$ absorber layer grown under low copper excess measured at 10 K. (b) Map of integrated PL yield over the marked P3 region (c) same map of integrated PL yield over the region of DA2 and (d) for DA1.

transition seen in low temperature PL measurements of CuGaSe$_2$ was first attributed to be a phonon replica [6], but later shown by spatially resolved PL [12] and CL [7] measurements, to be a third independent donor-acceptor pair transition (DA). From these findings and the similarity of PL spectra of CuInSe$_2$ and CuGaSe$_2$ [13] it was assumed that a peak seen at 0.94 eV in CuInSe$_2$ is also not a phonon replica but a third DA transition.

In the present study we carry out spatially resolved PL measurements at low temperatures on polycrystalline and epitaxial CuInSe$_2$ samples to review this assumption. Furthermore an additional distinct peak at 0.9 eV is detected in polycrystalline CuInSe$_2$ grown under high selenium overpressure. The peak is characterized with excitation and temperature dependent measurements. The same peak is also observed in Cu(In,Ga)Se$_2$ samples and its behavior with increasing [Ga]/([Ga] + [In])-ratio (GGI) is investigated. Admittance measurements on Schottky contacts are used as a complementary method to determine the activation energy. All samples studied are grown under copper excess, forming stoichiometric CuIn(Ga)Se$_2$ as well as a secondary Cu$_2$Se layer [14] which can be etched by potassium cyanide (KCN). The standard composition for high efficiency solar cells [Cu]/([Ga] + [In]) $\approx$ 0.9 cannot be used for defect spectroscopy via PL because they show strong compensation effects which distort the spectrum [4].

Methods

Polycrystalline samples are grown in a molecular beam epitaxy system in a co-evaporation process on molybdenum coated soda lime glass. For the ternary CuInSe$_2$ a one-stage process is used with constant elemental fluxes and constant temperature. The variation of growth conditions between processes is controlled by altering the copper flux as well as the selenium flux. The Cu(In,Ga)Se$_2$ samples are grown in a modified three-stage-process [15, 16], in which the duration of the third stage defines the overall [Cu]/([Ga] + [In])-ratio (CGI). The indium flux is varied to control the GGI. Roughly 600 nm thick epitaxial CuInSe$_2$ samples are grown by metal organic vapor phase epitaxy on undoped GaAs-wafers. Details about the growth process can be found elsewhere [6, 17, 18]. All samples are grown with a final Cu-rich composition, measured by energy dispersive x-ray spectroscopy (EDX) with 20 keV acceleration voltage. The EDX is measured on as grown samples including the Cu$_2$Se layer on top of the stoichiometric

bulk, since it is known that the copper overpressure influences the electronic structure of the bulk [5].

Spatially resolved PL measurements are performed in a home built confocal setup under continuous monochromatic excitation of an argon ion laser (514 nm) with a resolution of about 1 μm. More details about the optical setup can be found elsewhere [19]. Temperature dependent measurements are performed in a second setup where the emitted PL is collected by two off-axis mirrors and a diode laser (660 nm) is used for excitation. Both setups focus the collected PL into an optical fiber and use the same detection hardware. The light is spectrally resolved by a grating monochromator and measured by an InGaAs-detector array. A helium flow cryostat is used for temperature dependent measurements between 10 K and 300 K. Measured PL spectra are spectrally corrected and converted into energy space. For capacitance-voltage measurements as function of temperature (admittance measurements), bare-absorbers are etched with KCN to remove the copper selenide secondary phases and then aluminum is deposited to form a Schottky contact. Admittance spectra are recorded in a temperature range from 320 to 50 K and a frequency range of 100 Hz–1 MHz with an ac voltage amplitude of 30 mV rms using a closed-cycle helium cryostat under dark conditions.

Results and discussion

The photoluminescence spectrum measured at 10 K of a polycrystalline CuInSe$_2$ sample grown with low copper excess is shown figure 1(a). It shows the previously reported peaks for this composition at 1.035 eV, 0.99 eV and 0.97 eV [4, 12, 20, 21]. From temperature and excitation dependent PL measurements as well as other methods, the different peaks have been attributed to different kinds of transitions in literature. The main peak at 1.035 meV is related to excitonic luminescence [3, 4, 21–24]. The peak at 0.99 eV is assigned to a donor-acceptor pair transition (DA1) from a shallow donor (6–10 meV) to a shallow acceptor (40 meV) [3, 4, 20, 25–27]. The second defect related peak observed at 0.97 eV is the DA2 transition from the same donor into the second acceptor (60 meV) [3, 4, 22, 24]. In earlier publications [21, 23, 25] the peaks at 0.99 eV and 0.97 eV are attributed to free-bound transitions since the donor is really shallow. The third defect related peak at 0.94 eV (P3) has previously been attributed either to a phonon replica [4, 24] or to a third DA transition [5]. The attribution to a DA transition follows the shown third DA
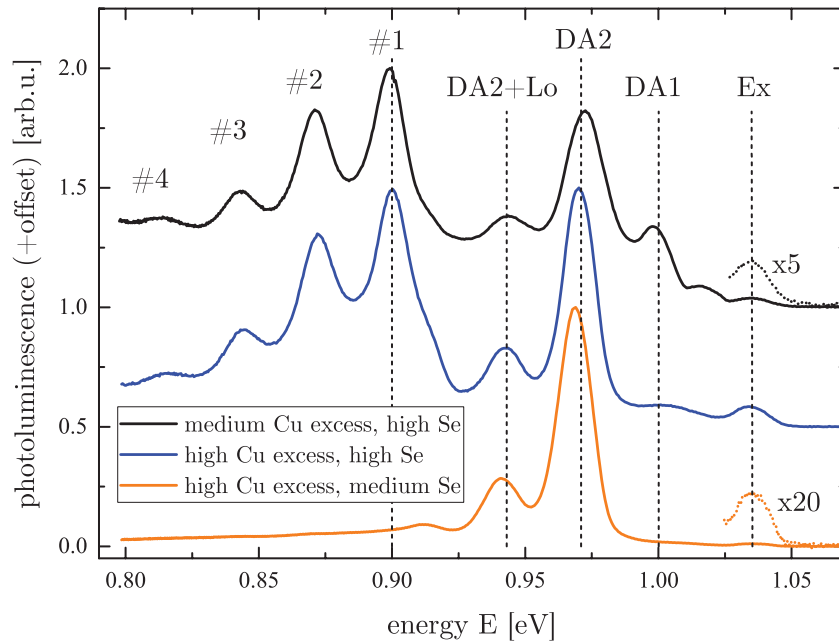
Figure 2. Measured photoluminescence spectra of polycrystalline CuInSe$_2$ absorber layer grown under high (blue, orange) and low Cu-excess (black) as well as high (black, blue) and low (orange) selenium flux measured at 10 K. The dotted black and orange lines depict a magnifications of the excitonic luminescence.

transition in CuGaSe$_2$ by CL [7] and by spatially resolved low temperature PL [12].

Similar spatially resolved low temperature PL measurements are carried out at 10 K on a polycrystalline CuInSe$_2$ sample in which for each position a full spectrum is recorded. For the evaluation of the spatial dependency, the spectra are integrated around each peak maximum as indicated in figure 1(a). The integrated PL intensity is plotted over the position for the third peak P3 in figure 1(b), the DA2 transition in (c) and the DA1 transition in (d). To compare the interdependency of the peaks the correlation coefficient is calculated as shown in [12] (see also supplementary materials EQ1 (stacks.iop.org/JPhysCM/31/425702/mmedia)). A weak correlation between the DA2 and DA1 transition of 0.8 is found. This correlation can be explained by a fluctuating photoluminescence intensity across the sample which affects the intensity of both DA2 and DA1. This intensity patterns have been reported earlier [19, 28] and lead to this weak correlation coefficient although both are not correlated. Comparing P3 and DA2 a high correlation coefficient of 0.96 is calculated, meaning that the PL yield of both peaks is fully dependent on each other in this sample.

Earlier investigation of epitaxial CuGaSe$_2$ samples showed an independent peak at lower energies (1.6 eV) than the DA2 transition (1.625 eV) which was attributed to a third DA transition (correlation coefficient 0.3) [12]. However, this peak could only be shown to be independent for samples grown with low excess (1 > [Cu]/[Ga] > 1.1). To verify if P3 is independent for a certain compositions the same analysis is carried out on a wide range of polycrystalline and epitaxial CuInSe$_2$ samples with various [Cu]/[In]-ratios (see supplementary materials S1 for an exemplary evaluation of a sample grown with high Cu-excess). On average the cross correlation coefficient between the DA2 and P3 is 0.95 and the lowest value

measured is 0.75. Probing the small [Cu]/[III] range, were the peak was found to be independent in CuGaSe$_2$, yields the same result. Overall, no evidence for an independent transition at 0.94 eV could be found in any sample. Also the temperature and intensity dependent behaviour of P3 and the DA2 agree well with each other and the energetic distance between P3 and DA2 fits to the reported phonon energy of CuInSe$_2$ [4, 22–24]. All this strongly indicates that the peak at 0.94 eV in CuInSe$_2$ is indeed a phonon replica of the DA2 transition.

However for certain polycrystalline samples another peak at lower energies was observed. To investigate this peak in more detail several polycrystalline CuInSe$_2$ samples with [Cu]/[In]-ratios between 1 and 2.5 as well as various selenium over-pressures were grown and their PL spectra measured at 10 K. For an exemplary sample grown under high copper excess, as shown in orange at the bottom of figure 2, the known peaks related to excitonic luminescence and the DA2 transition with phonon replica are found. The blue curve of figure 2 shows a sample grown with a similar copper excess but a higher selenium overpressure. This sample shows the characteristic excitonic peak as well as the DA2 transition with phonon replica. But additionally it has a distinct peak at 0.9 eV (#1) as well as peaks with decreasing PL yield towards lower energies (#2–4). First reported in [25], the peak at 0.9 eV (#1) was only mentioned or detected occasionally thereafter [21, 23, 24, 26, 29, 30]. If it was discussed, it was usually assigned to a free-to-bound transition (FB) or donor-acceptor-pair transition.

From excitation dependent measurements it is possible to extract the shift of the peak position β and the power law exponent k [31, 32]. For a DA transition k-values below 1 and a shift of a few meV/decade are expected [31] if the sample shows only weak compensation effects and has no deep defects [33]. For the sample with high Cu-excess and high Se excess (blue curve in figure 2), the DA2 transition and
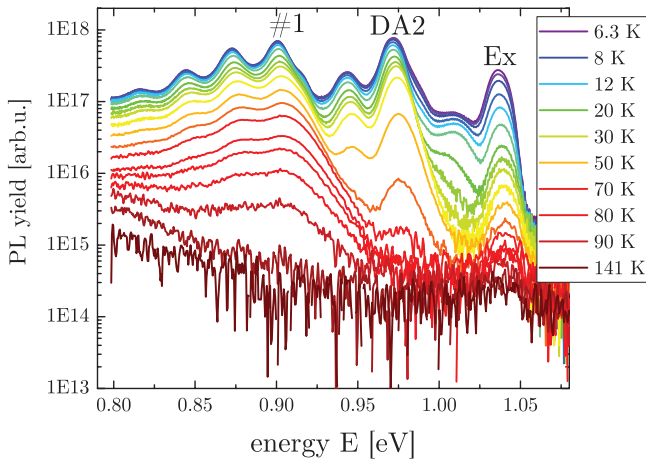
Figure 3. Temperature dependent photoluminescence measurements between 6 K and 141 K of a CuInSe$_2$ sample grown under high Cu-excess and a high selenium flux. The legend shows only every other temperature used.

its phonon replica show low excitation dependent shifts β of 0.7 meV/decade and k-values of 0.8 are determined. Peak #1 at 0.9 eV shows a similar k-value (0.7) and similar shift with excitation (0.5 meV/decade), making it likely to be another DA or FB transition. The peaks #2–4 show the same behaviour with excitation as peak #1 and can thus be identified as phonon replicas of it (see supplementary materials table 2 for detailed values). The energy difference between the peaks of 28 meV corresponds to the phonon energy of the DA2 transition and is in good agreement to the energy of the LO-phonon energy reported [4, 22–24].

A Huang–Rhys factor S of 0.35 is determined for the DA1 transition by fitting the line shape according to equation A4 of [34] (or see supplementary materials EQ2) which indicates a weak electron-phonon coupling. For peak #1 and its phonon replica a higher factor S of 0.75 is found showing a slightly stronger but still weak electron-phonon coupling. An exemplary fitting for the extraction of the Huang–Rhys factor can be found in the supplementary materials. The excitonic luminescence has a k value of 1.3 which is in good agreement with the expected value of $1 < k < 2$. If the Cu-excess during growth is lower but the selenium pressure remains high, a similar PL spectrum is measured (see black curve figure 2). In addition to the peaks already discussed, a new peak at 0.99 eV is observed corresponding to the DA1. Testing a variety of growth conditions no trend between Cu-excess and the appearance of the peak at 0.9 eV is found.

Temperature dependent measurements allow to study the thermal quenching of the different transitions and extract their activation energy E_A. Figure 3 shows the PL spectra of the sample with high Cu-excess (blue curve in figure 2) measured between 6 K and 140 K. The intensity of all observed transitions decreases with increasing temperature and the peak width of the defect related transitions (#1 and DA2) increases. The excitonic luminescence shows the strongest quenching as expected due to the low binding energy. The DA2 transition shows a slower quenching and peak #1 an even slower one.

The spectra are fitted as a whole to extract the PL yield which is plotted semi-logarithmically over the inverse temperature on the left side of figure 4. The data is fitted with a quenching model as described in [31, 32] (see also EQ3 in the supplementary materials). The excitonic luminescence shows an activation energy of roughly 5 meV agreeing well with literature values reported [3]. Evaluating the DA2 transition yields a shallow defect (below 8 meV) and a deeper defect of (66 ± 5) meV in agreement with literature values [4, 22, 24]. The same evaluation for peak #1 yields a similar shallow defect and a deeper defect with an activation energy of (135 ± 9) meV.

By plotting the position of the peak maximum over the temperature, as shown on the right in figure 4, it can be seen that both curves show exactly the same blue shift of 0.09 meV K^{-1} between 12 and 60 K. In case of the DA2 transition this shift has been interpreted as the change from a DA transition into a free-to-bound transition (FB) [4] due to thermal emptying of the shallower defect by emission of the trapped carrier to the band edge. For the DA2 transition this shallower defect is known to be the involved donor. From the identical shift of the peak maxima with temperature as well as similar activation energies for the shallow defect, it is concluded, that the same donor level is involved in both transitions and that peak #1 is a DA transition involving a third acceptor A3. With the attribution to a DA-transition also the broadening of the DA3 with increasing temperature can be explained by the already discussed gradual changed of the DA to a FB-transition with increasing temperature.

The activation energy E_{DA3} determined from temperature dependent measurements was measured for samples grown with various Cu-excess and found to scatter between 110 meV and 145 meV. The scattering originates from the strong influence of the few data points at higher temperatures onto the fitting routine. Another way to verify the activation energy of a transition is to look at the energy difference between the respective peak and the excitonic transition. The energy of the excitonic transition represents the band gap energy, reduced by the excitonic binding energy, whereas the DA transition is determined by the band gap energy, reduced by the activation energies of the donor and the acceptor as well as the Coulomb energy [35]. The energetic distance between the two peaks can be directly interpreted as the activation energy of the acceptor, since the binding energy of the exciton and the activation energy of the involved donor in the DA transition are both in the range of 5–10 meV [3, 4, 32]. The Coulomb energy can be neglected since the measurements were performed at low excitation densities and due to the low Coulomb shifts expected for materials grown with Cu-excess. With this method all samples show a concurrent activation energy of (135 ± 10) meV.

The origin of the third acceptor A3 is unknown and will be discussed in the following. Plotting the ratio of the peak heights (DA3/DA2) over the copper excess used during growth (see supplementary materials S3), no clear trend is found. In the range of $1 < $ Cu/In $ < 1.8$ the DA3/DA2-ratio scatters randomly between 0.05 and 1.5. With increasing copper content,
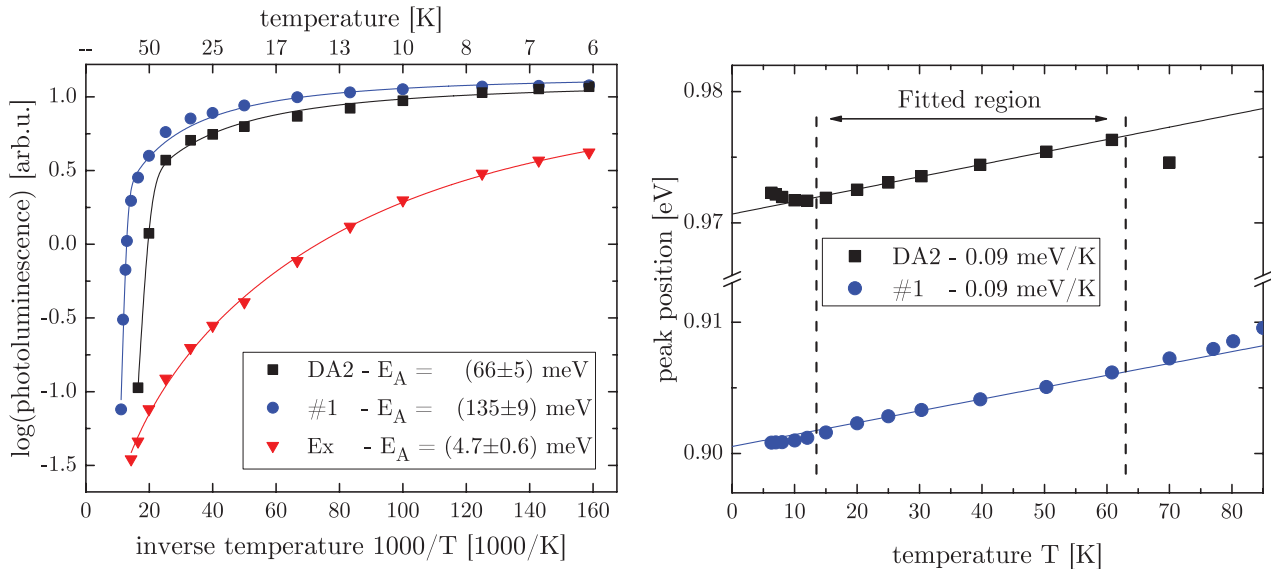
Figure 4. Left: semi-logarithmic plot of the PL yield over the inverse temperature for the extraction of the activation energy E_A of the DA2 transition (blue), peak #1 (black) and the excitonic luminescence (red). Right: peak position of the DA2 transition (black) and peak #1 (blue) plotted over the temperature.

the highest DA3/DA2-ratio observed decreases but this could also be related to the smaller sample size in this compositional region. More pronounced is the correlation between the DA3/DA2 ratio and the temperature of the cracking head of the selenium source. In the past the baseline process in our lab would use a temperature of 600 °C. Those samples show no or low contributions of the DA3 transition in low temperature PL measurements. The current baseline process uses 1000 °C and the DA3 is seen in almost all samples. It is thus argued that the selenium overpressure and the selenium species which changes with the temperature of the cracking head [36, 37] have a strong influence on the formation likelihood of the defect responsible the third acceptor.

Theoretical calculations by Pohl and Albe [38] find that the indium vacancy (V_{In}) is supposed to be a shallow acceptor type defect in CuInSe$_2$. Also other recent calculations using the screened-exchange hybrid density functional theory of Heyd, Suseria and Ernzerhof (HSE06) show that V_{In} is a more or less shallow acceptor type defect [39–42]. Looking at the formation energy of this defect for different growth condition could explain why this defect is only observed occasionally. The formation energy of V_{In} decreases with increasing chemical potential of selenium [38], making the formation more likely. This would explain why this defect is not observed in epitaxial samples grown by MOCVD [3, 4] but seen in polycrystalline samples grown by co-evaporation [24] and single crystals [21]. During the MOCVD growth process the availability of reactive selenium is low since the metal organic precursor only starts to decompose near growth temperature. On the other side during the growth by co-evaporation high selenium overpressure are used (about 20× the needed selenium) and the single crystal showing the DA3 was annealed in the presence of excess selenium [21].

Another possible origin could be a defect complex as discussed by Malitckaya *et al* [42]. From the three complexes discussed the one formed by an copper interstitial Cu$_i$ together

with a copper on indium antisite Cu$_{In}$ has the lowest formation energy. But it is only an acceptor type defect for n-type materials, which is not the case for the grown samples. A second complex formed by Cu$_i$ and V_{In}, is an acceptor type defect in p-type material, but has a high formation energy than V_{In} alone. Because of this we think it is unlikely that the A3 is related to this complex. The third complex is formed by Cu$_i$ and V_{Cu} which are both abundant in samples grown with low and moderate Cu-excess. But the complex has a low binding energy and is thus likely to dissociate. However, it is plausible that it exist because of the high concentration of constituents. Of the proposed defect complexes this is the only potential candidate that is plausible from our point of view. However, comparing the defect complex and V_{In} the latter one seems more likely and is thus proposed as a possible origin of the acceptor defect in the ternary CuInSe$_2$.

The DA1 transition exist over the whole range of solid solution of Cu(In,Ga)Se$_2$ [3] and the same has been proposed for the DA2 transition. To validate the same for the DA3, the Cu(In,Ga)Se$_2$ growth process is adjusted to promote the presence of the DA3. It should be noted here that the Cu(In,Ga)Se$_2$ samples grown by a three-stage process have a lower lateral variation in thickness and a lower surface roughness, compared to the CuInSe$_2$ samples grown by the one-stage process. The combination of both effects leads to interference effects in the wavelength region of the emitted PL as determined by reflectance measurements. Those interference fringes distort the PL spectra especially at low energies [43, 44] and prohibit a quantitative analysis of the data. To remove the interference effects a scattering layer is deposited, as shown in [45], in order to change the reflectivity of the surface. Reflectance measurements after the surface modification confirm the removal of the interference fringes. See supplementary materials for exemplary reflectance and PL measurements of a sample with and without a scattering layer.
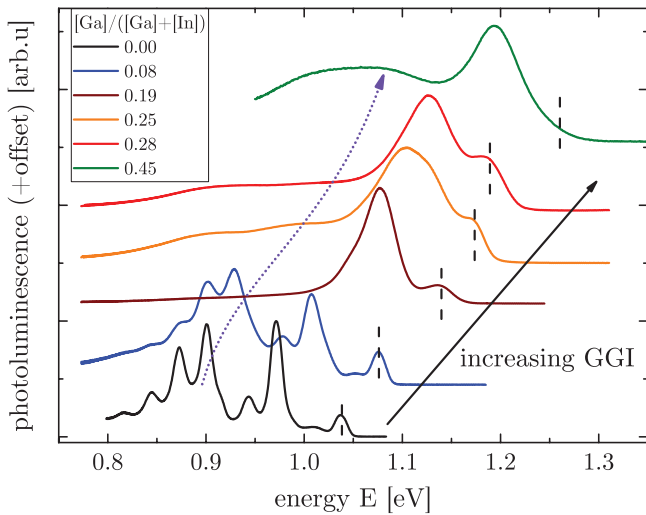
Figure 5. Measured photoluminescence spectra of $Cu(In,Ga)Se_2$ absorber layers grown under Cu-excess with increasing gallium content at 10 K. The dashed vertical lines indicate the position of the excitonic luminescence. The dotted purple line indicates the shift of the DA3 transition.

Figure 6. Peak position of the different transitions observed in $Cu(In,Ga)Se_2$ with various GGI plotted over the peak position of the exciton as a measure of gallium content. The data for $CuGaSe_2$ is taken from [6]. The solid lines depict linear fits through the data. The dashed lines estimate the peak shift of the two peaks at low energies with higher gallium content.

Low temperature PL spectra under similar illumination conditions for various $Cu(In,Ga)Se_2$ samples with GGI-ratios ranging from 0 to 0.45 are shown in figure 5. The energetic position of the exciton, indicated by the dashed vertical black line, increases with the incorporation of gallium and follows the bandgap. For the lowest GGI value of 0.08 both the DA2 and the DA3 with their respective phonon replica are clearly identified. The energetic position is shifted to higher energies showing that the involved shallow defects follow the band edges. For higher GGI values all peaks broaden due to the inherent compositional fluctuations of indium and gallium within the absorber layer. The DA3 transition is less pronounced in the $Cu(In,Ga)Se_2$ samples, but the respective position can be tracked as shown by the dotted purple line.

For GGI values above of 0.25 two peaks at low energies (0.87 eV and 0.97 eV) are observed (see semi-logarithmic plot in the supplementary materials S5 for better distinction). Since inference can be excluded and the double peak structure is observed in all samples with higher GGI, it is concluded that two different transition are observed. All spectra are fitted as a whole with Gaussian profiles and the known line shape for the phonon replicas [34]. The extracted position of the respective peaks is plotted over the position of the excitonic luminescence in figure 6. The position of the excitonic luminescence is chosen as the x-axis value since it is a good indicator for the local GGI of the probed sample, whereas the values determined by EDX are averaged over a large area and have a limited accuracy. For comparison the data of a $CuGaSe_2$ sample is added, taken from [6]. All peaks shift towards higher energies with the addition of gallium. A linear fit through the data points of the DA1 and DA2 transition yield a good fit over the whole GGI range and indicate the existence of the DA2 over the full compositional range. The DA3 transition shifts weaker with the addition of gallium compared to the DA1 and DA2 transition, which means that the A3 acceptor shifts deeper into the bandgap. For the second
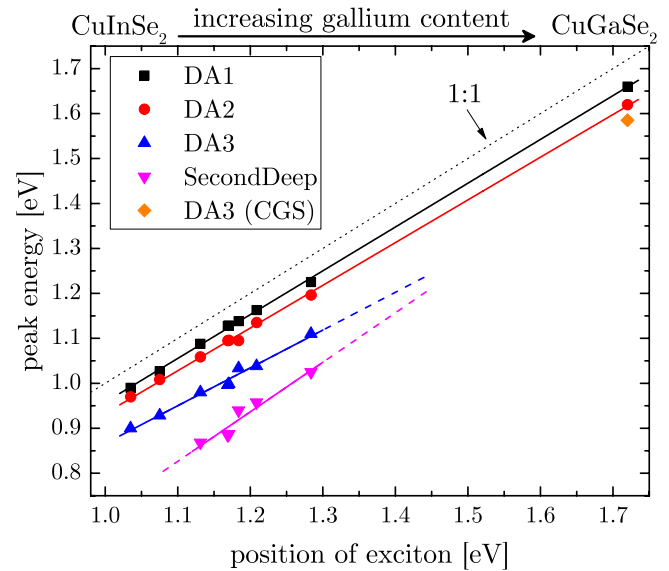
deep transition the opposite is observed. If the trend continues for GGI values between 0.5 (1.35 eV) and 0.9 (1.63 eV), both peaks will likely merge together and will be not distinguishable anymore.

The straight forward way to discuss the second peak at low energies would be as the gallium vacancy (V_{Ga}). But indium and gallium share the same position in the $Cu(In,Ga)Se_2$ lattice and are known to be without any order. Whether an indium or gallium atom is missing, does not play role and the related defect is V_{III}, which energetic defect level is defined by the next neighboring III atoms (indium and/or gallium). There are five possible configurations of In and Ga around a V_{III} ($4 \times In$, $3 \times In$ and $1 \times Ga$, $2 \times In$ and $2 \times Ga$, $1 \times In$ and $3 \times Ga$, $4 \times Ga$). With increasing gallium content the most likely configuration would change more or less linear. As it is not likely that different next shell configurations lead to a distinct second peak, this change between configuration will lead to one smeared out broad peak. Which fits to the data as a stronger broadening of the DA3 compared to the DA2 transition is observed. We can therefore not conclude on the nature of the defect involved in the second deep transition. On a short side notice, due to the different growth conditions required for the DA3 in $CuInSe_2$ and $Cu(In,Ga)Se_2$ (high selenium, no dependance on Cu-excess) and of the DA3 in $CuGaSe_2$ (low selenium, low Cu-excess required) as well as the non fitting extrapolation of the activation energy between both, it is argued that both defects originate from different defect (complexes). In the future they should thus be carefully distinguished to avoid misconceptions.

To verify the found trends of the activation energy complementary admittance measurements [46] are conducted. For this the absorber layers were etched and aluminum was deposited to form a Schottky contact. The ternary $CuInSe_2$ samples were annealed under selenium atmosphere before
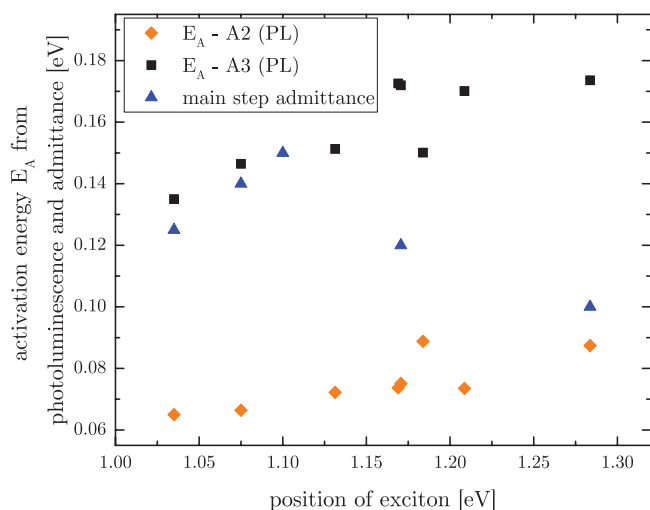
Figure 7. Activation energy of the second acceptor A2 (orange) and the A3 defect (black) from photoluminescence measurements at 10 K as well as the activation energy of the main capacitance step from admittance measurements (blue) plotted over the energy position of the excitonic luminescence.

the deposition of the front contact to remove a surface defect [47, 48]. The measured admittance spectra are dominated by one main capacitance step, whose activation energy is extracted from an Arrhenius plot of the inflections points (see supplementary materials S6 and S7 for admittance spectra and Arrhenius plots). For $CuInSe_2$, an activation energy of about 125 meV was extracted which matches with the 135 meV activation energy of the A3 defect determined by PL. In figure 7, the activation energy of the A2 defect and the A3 defect found by low temperature PL as well as the activation energy of the main admittance step are plotted over the energetic position of the excitonic luminescence of the respective sample. The activation energy from admittance agrees well with the activation energy of the A3 defect for low gallium contents. Based on that, we can conclude that the same defect is observed in both methods, linking optical and electrical measurement techniques. For GGI values above 0.15, the activation energy values from admittance decrease and approach the value of the A2 defect, whereas those from PL keep increasing. A possible explanation for the decrease is that the A3 defect does not dominate the admittance spectrum anymore, which is likely related to the defect moving deeper into the bandgap and possibly a reduced quantity of defect states.

Conclusion

Spatially resolved PL measurements show a clear correlation of the formally assigned 'DA3' transition at 0.94 eV to the DA2 transition at 0.97 eV found in $CuInSe_2$, strongly indicating that the peak is a phonon replica and not an independent DA transition. On the other hand in samples grown under high selenium overpressure a defect related peak at 0.9 eV can be identified in a broad range of copper over indium ratios. The peak was characterized by excitation and temperature dependent photoluminescence measurements and found to be a donor-acceptor pair transition (DA3) from a shallow donor

(<8 meV) into a shallow acceptor A3 (135 ± 10) meV. Peaks below 0.9 eV have been identified as phonon replica of the DA3 transition with a Huang–Rhys factor of 0.75 and an energy of the involved phonon of 28 meV. The defect formation seem to be independent of copper excess during growth but the use of highly reactive selenium (usage of cracking head at 1000 °C) favours the formation. The DA3 could also be identified in $Cu(In,Ga)Se_2$. Admittance measurements on Schottky contacts show a good agreement between the activation energy of the A3 defect and the activation energy of the main step of the capacitance measurements for low gallium contents. Both methods show an increasing activation energy with gallium content shifting the defect deeper into the bandgap. A possible origin for the A3 could be the indium vacancy (V_{In}) in $CuInSe_2$ and the III-vacancy (V_{III}) in $Cu(In,Ga)Se_2$.

ORCID iDs

Finn Babbe ⓘ https://orcid.org/0000-0002-9131-638X
Hossam Elanzeery ⓘ https://orcid.org/0000-0001-6032-2499
Max H Wolter ⓘ https://orcid.org/0000-0002-9202-7627
Susanne Siebentritt ⓘ https://orcid.org/0000-0001-6522-1427

References

[1] Jackson P, Wuerz R, Hariskos D, Lotter E, Witte W and Powalla M 2016 Effects of heavy alkali elements in Cu(In,Ga)Se₂ solar cells with efficiencies up to 22.6% *Phys. Status Solidi RRL* **10** 583–6
[2] Solar Frontier 2019 Solar Frontier achieves world record thin-film solar cell efficiency of 23.3% (http://www.solar-frontier.com/eng/news/2019/0117_press.html) (Visited on: 05 May 2019)
[3] Rega N, Siebentritt S, Albert J, Nishiwaki S, Zajogin A, Lux-Steiner M C, Kniese R and Romero M J 2005 Excitonic luminescence of Cu(In,Ga)Se₂ *Thin Solid Films* **480–1** 286–90
[4] Siebentritt S, Rega N, Zajogin A and Lux-Steiner M C 2004 Do we really need another PL study of CuInSe₂? *Phys. Status Solidi* c **1** 2304–10
[5] Siebentritt S, Gütay L, Regesch D, Aida Y and Deprédurand V 2013 Why do we make Cu(In,Ga)Se₂ solar cells non-stoichiometric? *Sol. Energy Mater. Sol. Cells* **119** 18–25
[6] Bauknecht A, Siebentritt S, Albert J and Lux-Steiner M C 2001 Radiative recombination via intrinsic defects in CuxGaySe₂ *J. Appl. Phys.* **89** 4391–400
[7] Siebentritt S, Beckers I, Riemann T, Christen J, Hoffmann A and Dworzak M 2005 Reconciliation of luminescence and

Hall measurements on the ternary semiconductor CuGaSe₂ *Appl. Phys. Lett.* **86** 1–3

[8] Krysztopa A, Igalson M, Aida Y, Larsen J K, Gütay L and Siebentritt S 2011 Defect levels in the epitaxial and polycrystalline CuGaSe₂ by photocurrent and capacitance methods *J. Appl. Phys.* **110** 103711

[9] Gerhard A, Harneit W, Brehme S, Bauknecht A, Fiedeler U, Lux-Steiner M C and Siebentritt S 2001 Acceptor activation energies in epitaxial CuGaSe₂ grown by MOVPE *Thin Solid Films* **387** 67–70

[10] Schuler S, Siebentritt S, Nishiwaki S, Rega N, Beckmann J, Brehme S and Lux-Steiner M C 2004 Self-compensation of intrinsic defects in the ternary semiconductor CuGaSe₂ *Phys. Rev.* B **69** 045210

[11] Spindler C, Babbe F, Wolter M H, Ehre F, Santosh K, Hilgert P, Werner F and Siebentritt S 2019 Electronic Defects in Cu(In,Ga)Se₂—towards a comprehensive model *Phys. Rev. Mater.* (under review)

[12] Larsen J K 2011 Inhomogeneities in epitaxial chalcopyrites studied by photoluminescence *PhD Thesis* University of Luxembourg

[13] Siebentritt S 2013 Why are kesterite solar cells not 20% efficient? *Thin Solid Films* **535** 1–4

[14] Gödecke T, Haalboom T and Ernst F 1948 Phase equilibria of Cu-In-Se I. The In₂Se₃-Se-Cu₂Se subsystem *Z. Met.kd.* **91** 622–34

[15] Gabor A M, Tuttle J R, Albin D S, Contreras M A, Noufi R and Hermann A M 1994 High-efficiency CuInxGa₁-xSe₂ solar cells made from (Inx,Ga₁-x)₂Se₃ precursor films *Appl. Phys. Lett.* **65** 198–200

[16] Choubrac L, Bertram T, Elanzeery H and Siebentritt S 2017 Cu(In,Ga)Se₂ solar cells with improved current based on surface treated stoichiometric absorbers *Phys. Status Solidi* a **214** 1600482

[17] Gütay L, Larsen J K, Guillot J, Müller M, Bertram F, Christen J and Siebentritt S 2011 MOVPE of CuGaSe₂ on GaAs in the presence of a CuxSe secondary phase *J. Crystal Growth* **315** 82–6

[18] Spindler C, Regesch D and Siebentritt S 2016 Revisiting radiative deep-level transitions in CuGaSe₂ by photoluminescence *Appl. Phys. Lett.* **109** 032105

[19] Larsen J K, Gütay L and Siebentritt S 2011 Influence of secondary phase CuxSe on the optoelectronic quality of chalcopyrite thin films *Appl. Phys. Lett.* **98** 201910

[20] Rincón C, Bellabarba C, González J and Sánchez Pérez G 1986 Optical properties and characterization of CuInSe₂ *Sol. Cells* **16** 335–49

[21] Mudryi A V, Bodnar I V, Gremenok V F, Victorov I A, Patuk A I and Shakin I A 1998 Free and bound exciton emission in CuInSe₂ and CuGaSe₂ single crystals *Sol. Energy Mater. Sol. Cells* **53** 247–53

[22] Yu P W 1976 Radiative recombination in melt-grown and Cd-implanted CuInSe₂ *J. Appl. Phys.* **47** 677–84

[23] Niki S, Makita Y, Yamada A, Obara A, Misawa S, Igarashi O, Aoki K and Kutsuwada N 1994 Sharp optical emission from CuInSe2 thin films grown by molecular beam epitaxy *Japan. J. Appl. Phys.* **33** L500–02

[24] Wagner M, Dirnstorfer I, Hofmann D M, Lampert M D, Karg F and Meyer B K 1998 Characterization of CuIn(Ga) Se₂ thin films I. Cu-Rich layers *Phys. Status Solidi* a **167** 131–42

[25] Massé G and Redjai E 1984 Radiative recombination and shallow centers in CuInSe₂ *J. Appl. Phys.* **56** 1154–9

[26] Abou-Elfotouh F, Dunlavy D, Cahen D, Noufi R, Kazmerski L and Bachmann K 1984 Photoluminescence studies of CuInSe₂: identification of intrinsic defect levels *Prog. Cryst. Growth Charact.* **10** 365–70

[27] Dagan G, Abou-Elfotouh F, Dunlavy D J, Matson R J and Cahen D 1990 Defect level identification in copper indium selenide (CuInSe₂) from photoluminescence studies *Chem. Mater.* **2** 286–93

[28] Gütay L and Bauer G 2009 Local fluctuations of absorber properties of Cu(In,Ga)Se₂ by sub-micron resolved PL towards 'real life' conditions *Thin Solid Films* **517** 2222–5

[29] Chatraphorn S, Yoodee K, Songpongs P, Chityuttakan C, Sayavong K, Wongmanerod S and Holtz P O 1998 Photoluminescence of a high quality CuInSe2 single crystal *Japan. J. Appl. Phys.* **37** L269–71

[30] Yakushev M, Feofanov Y, Martin R, Tomlinson R and Mudryi A 2003 Magneto-photoluminescence study of radiative recombination in CuInSe₂ single crystals *J. Phys. Chem. Solids* **64** 2011–6

[31] Rau U and Siebentritt S 2006 *Wide-Gap Chalcopyrites* (*Springer Series in Materials Science* vol 86) ed S Siebentritt and U Rau (Berlin: Springer)

[32] Unold T and Gütay L 2011 Photoluminescence analysis of thin-film solar cells *Advanced Characterization Techniques for Thin Film Solar Cells* vol 1–2, ed D Abou-Ras *et al* (Weinheim: Wiley) pp 151–75

[33] Spindler C, Rey G, Galvani T, Wirtz L and Siebentritt S 2018 Excitation-intensity dependence of shallow and deep-level photoluminescence transitions in semiconductors *J. Appl. Phys.* (under review)

[34] Alkauskas A, McCluskey M D and Van de Walle C G 2016 Tutorial: defects in semiconductors—combining experiment and theory *J. Appl. Phys.* **119** 181101

[35] Pankove J I 1975 *Optical Processes in Semiconductors* (New York: Dover)

[36] Rau H 1974 Vapour composition and critical constants of selenium *J. Chem. Thermodyn.* **6** 525–35

[37] Viswanathan R, Balasubramanian R, Darwin Albert Raj D, Sai Baba M and Lakshmi Narasimhan T 2014 Vaporization studies on elemental tellurium and selenium by Knudsen effusion mass spectrometry *J. Alloys Compd.* **603** 75–85

[38] Pohl J and Albe K 2013 Intrinsic point defects in CuInSe₂ and CuGaSe₂ as seen via screened-exchange hybrid density functional theory *Phys. Rev.* B **87** 245203

[39] Oikkonen L E, Ganchenkova M G, Seitsonen A P and Nieminen R M 2014 Formation, migration, and clustering of point defects in CuInSe₂ from first principles *J. Phys.: Condens. Matter* **26** 345501

[40] Bekaert J, Saniz R, Partoens B and Lamoen D 2014 Native point defects in CuIn₁-xGaxSe₂: hybrid density functional calculations predict the origin of p- and n-type conductivity *Phys. Chem. Chem. Phys.* **16** 22299–308

[41] Yee Y S, Magyari-Köpe B, Nishi Y, Bent S F and Clemens B M 2015 Deep recombination centers in Cu₂ZnSnSe₄ revealed by screened-exchange hybrid density functional theory *Phys. Rev.* B **92** 195201

[42] Malitckaya M, Komsa H-P, Havu V and Puska M J 2017 First-principles modeling of point defects and complexes in thin-film solar-cell absorber CuInSe₂ *Adv. Electron. Mater.* **3** 1600353

[43] Larsen J K, Li S-Y, Scragg J J S, Ren Y, Hägglund C, Heinemann M D, Kretzschmar S, Unold T and Platzer-Björkman C 2015 Interference effects in photoluminescence spectra of Cu₂ZnSnS₄ and Cu(In,Ga)Se₂ thin films *J. Appl. Phys.* **118** 035307

[44] Wolter M H, Bissig B, Reinhard P, Buecheler S, Jackson P and Siebentritt S 2017 Correcting for interference effects in the photoluminescence of Cu(In,Ga)Se$_2$ thin films *Phys. Status Solidi* c **14** 1600189

[45] Wolter M H, Siopa D, Thiele P, Dale P, Avancini E, Bissig B, Carron R, Buecheler S and Siebentritt S 2019 Applying a surface treatment to chalcopyrite thin films to eliminate interference effects (in preparation)

[46] Heath J and Zabierowski P 2011 Capacitance spectroscopy of thin-film solar cells *Advanced Characterization Techniques for Thin Film Solar Cells* ed D Abou-Ras *et al* (Weinheim: Wiley) pp 81–105

[47] Elanzeery H, Melchiorre M, Sood M, Babbe F, Werner F, Brammertz G and Siebentritt S 2019 Challenge in Cu-rich CuInSe$_2$ thin film solar cells: defect caused by etching *Phys. Rev. Mater.* **3** 055403

[48] Babbe F, Elanzeery H, Melchiorre M, Zelenina A and Siebentritt S 2018 Potassium fluoride postdeposition treatment with etching step on both Cu-rich and Cu-poor CuInSe$_2$ thin film solar cells *Phys. Rev. Mater.* **2** 105405